Electronic Supplementary Material (ESI) for Materials Advances.

Electronic Supplementary Information (ESI):

Unveiling the Role of Electrode Polarization in Modulating Dielectric and Electro-Optical Properties of SnSe Dispersed Nematic Liquid Crystal

Bhupendra Pratap Singh[a], Piyush Mishra[b], Mohammad Rafe Hatshan[c], Dharmendra Pratap Singh[d] and Shug-June Hwang[a,*]

[a]Department of Electro-Optical Engineering, National United University, Miao-Li-360, Taiwan.
[b]CSIR-National Physical Laboratory, Dr. K.S. Krishnan Marg, New Delhi-110012, India.
[c]Department of Chemistry, College of Science, King Saud University, Riyadh, 11451 Saudi Arabia.
[d]Université du Littoral Côte d'Opale, UR 4476, UDSMM, Unité de Dynamique et Structure des Matériaux Moléculaires, Calais 62228, France.
[*]Author to whom any correspondence should be addressed:
Email: june@nuu.edu.tw

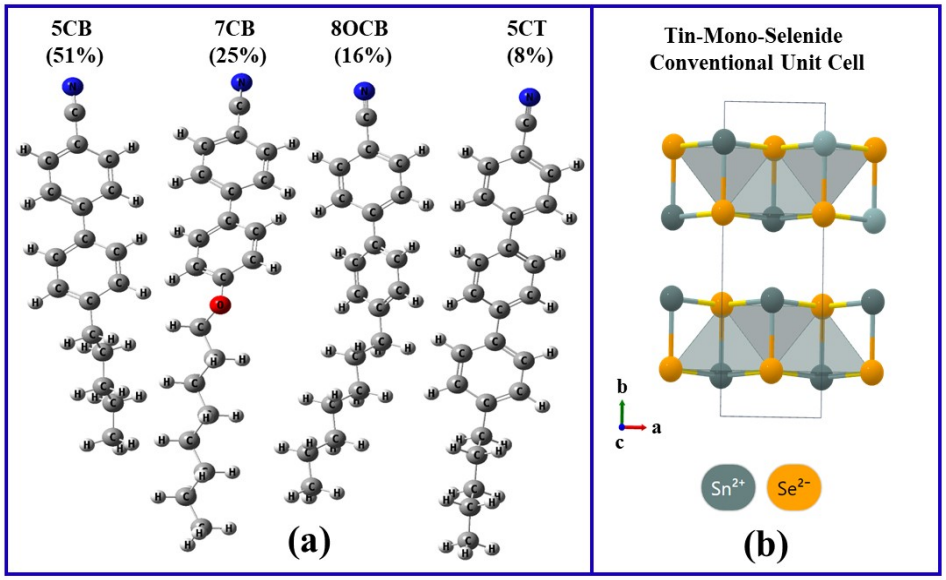

Figure S1: (a) Molecular structure of E7 LCs, and (b) conventional unit cell of SnSe; crystallizes in the orthorhombic Pnma space group.

Measurement Methods:

In this research study, we conducted frequency-dependent dielectric and capacitance measurements on LC/SnSe NSs composite systems. These measurements were carried out in both planar and homeotropically oriented cells. We used a Solartron (SL-1260) to measure the complex dielectric permittivities in a frequency range of 10 Hz to 5.5 MHz. The measurements

were performed under an applied alternating field of 0.01 V/μm. The obtained data included the storage component (real part) ε' and the loss component (imaginary part) ε'' of the complex dielectric permittivities, as well as the dielectric anisotropy.

Additionally, we determined the pretilt angle and rotational viscosity (γ) of both pristine and SnSe-dispersed LC cells. To achieve this, we employed the crystal rotation method and transient current methods. [1,2] Overall, these investigations provided us with important insights into the electrical characteristics and behavior of LC/SnSe composite systems, providing light on their prospective applications in various electronic devices.

Employing the provided experimental configuration, the voltage-dependent transmittance (V-T Curve) for both pristine and SnSe-blends was evaluated. A 10 mW helium-neon (He-Ne) laser emitting at a wavelength of 632.8 nm was projected orthogonally onto the sample cell, its intensity modulated by a neutral-density (ND) filter. The applied voltage waveform comprised a 1 kHz square wave. Positioned at a 45° angle with respect to the transmission axis of the polarizer and the cell's rubbing direction, the sample cell was situated between two crossed polarizers.

To investigate the electro-optical dynamic response, we utilized specific equipment and methods in this research study. First, we generated a carrier signal with a frequency of 1 kHz and an amplitude of 20V using a Tektronix AFG3022 signal generator. A 50 mHz square wave was used to modify the carrier signal. We used a high-speed photodiode with a reaction time of 100 microseconds to measure the intensity of the transmitted light. To reduce statistical noise, the detected signal was captured on a Tektronix TDS 2014 digital oscilloscope and averaged across 32 measurements. We were able to characterize the optical properties of both pure LC and LC blended with SnSe by examining the resulting V-T Curve.

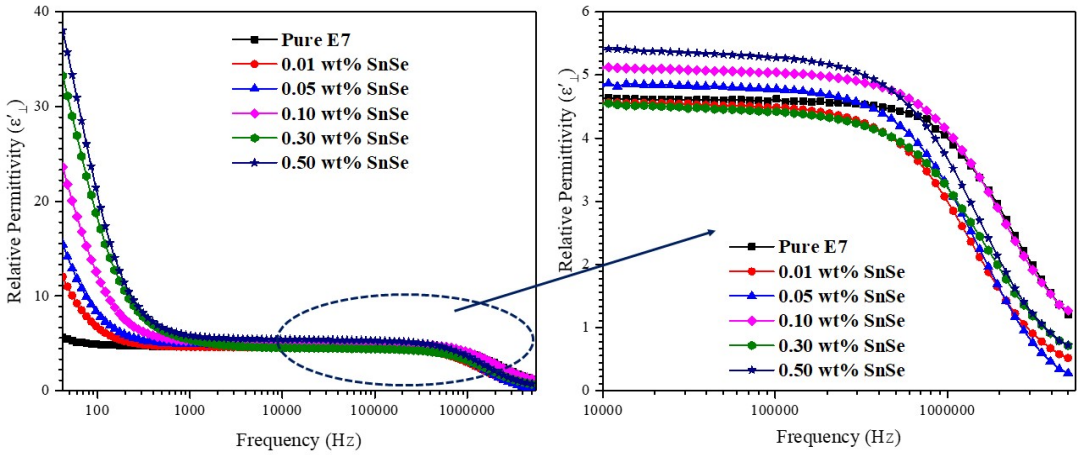

Figure S2: Dielectric permittivity with the function of the frequency for pure and nano liquid crystal composites at room temperature (ECB or HA Mode).

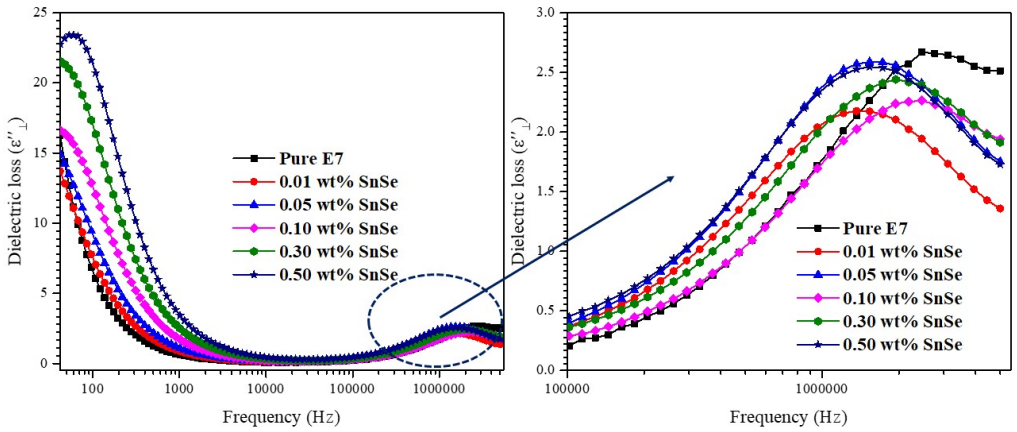

Figure S3: Dielectric loss with the function of the frequency for pure and nano liquid crystal composites at room temperature (ECB or HA Mode).

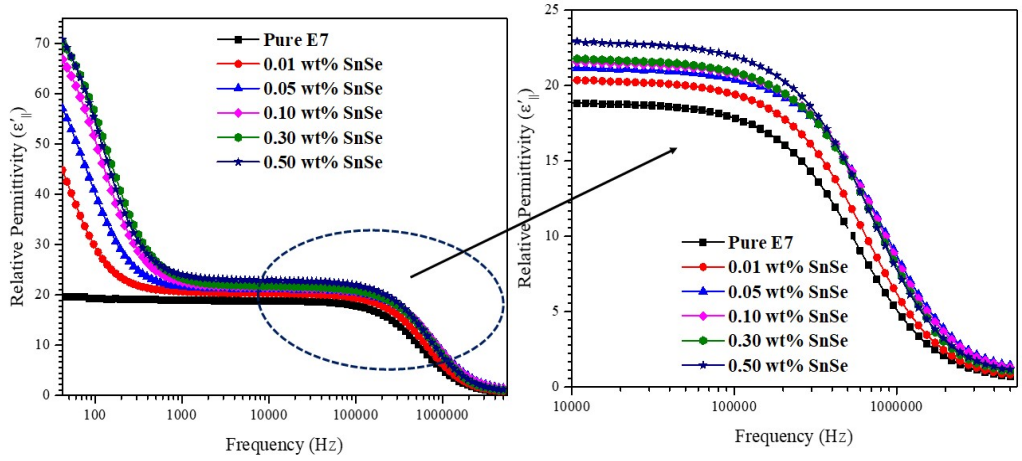

Figure S4: Dielectric permittivity with the function of the frequency for pure and nano liquid crystal composites at room temperature (VA Mode).

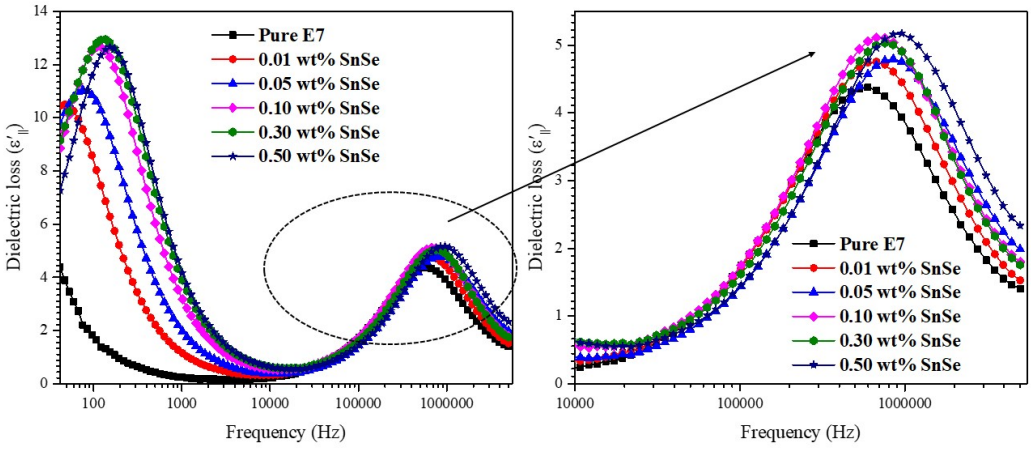

Figure S5: Dielectric loss with the function of the frequency for pure and nano liquid crystal composites at room temperature (VA Mode).

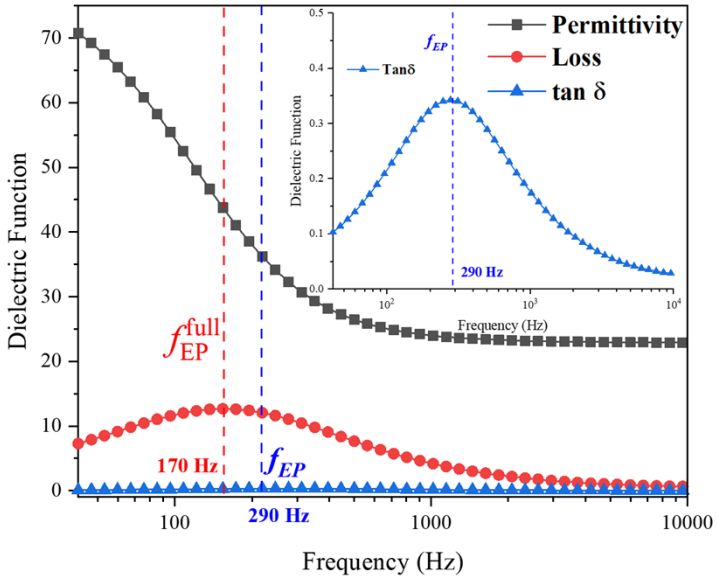

Figure S6: Permittivity spectrum of a dispersion containing 0.5% SnSe nanospheres (NSs) in pure E7 LC, demonstrating the characteristics of dielectric permittivity components ($\varepsilon_{\perp}$ & $\varepsilon_{\parallel}$) and $\tan\delta$ in the presence of electrode polarization (VA Mode). The initiation frequency of electrode polarization (f_{EP}) is determined by the peak value of tan delta, while the frequency at which it fully develops (f_{EP}^{full}) corresponds to the maximum dielectric loss. Furthermore, a substantial increase of more than two-fold is observed in the perpendicular component of dielectric permittivity within this range.

Ion Trapping Mechanism:

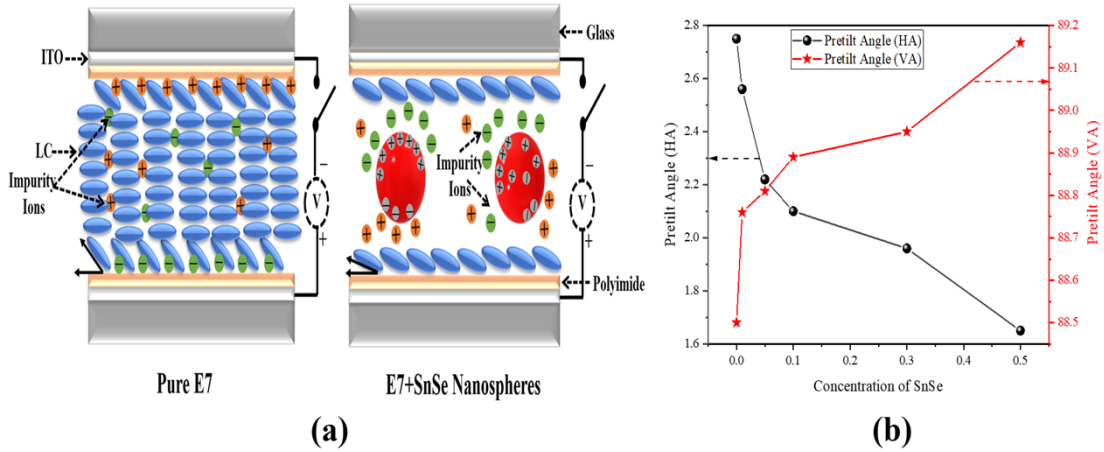

Figure S7: (a) Scientific illustration depicting the functioning of the NLC molecule-interaction with alignment layers. The mechanism underlying the formation and reduction of pretilt angle is elucidated. Intermittent electrification of SnSe NSs by specifically charged ionic impurities leads to the accumulation of charged NSs within NLC molecules. Consequently, the charged ionic impurities are driven away from the alignment layer and gather around SnSe NSs in the absence of an applied voltage. This molecular interaction between electrically charged SnSe NSs and ionic impurities strengthens van der Waals

dispersion interactions between NLC molecules and the alignment layers, resulting in a decrease in the pretilt angle. (b) variation of pretilt angles of homogeneously aligned (HA) and vertically aligned LC cells with various SnSe NS concentrations.

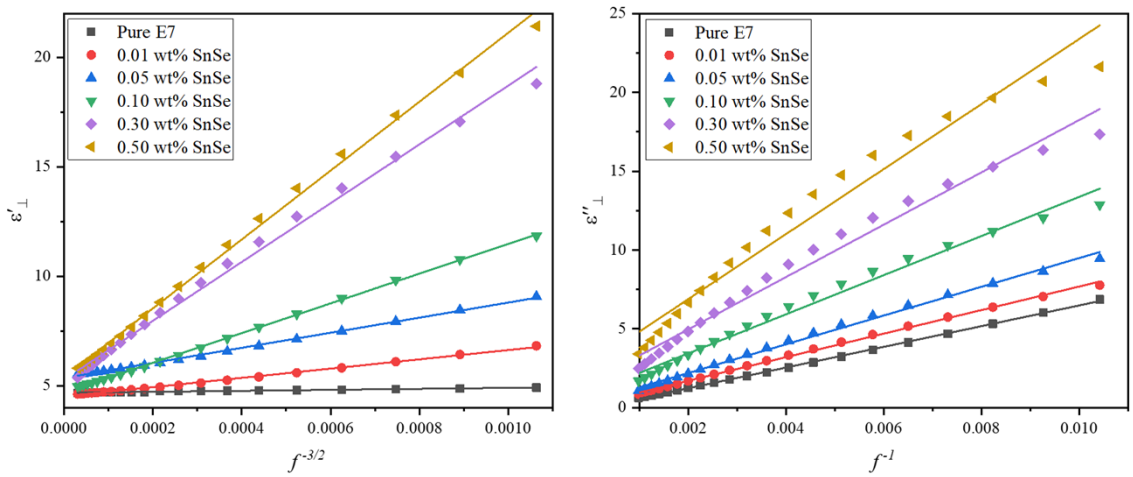

Figure S8: The linear fitting of the experimental data of the corresponding (a) dielectric permittivity and (b) dielectric loss of the E7 LC at different doping concentrations of SnSe NSs at RT.

The Uemura model has been employed to examine the effect of ionic impurities on the dielectric spectra (see Figure S8). This model can be expressed as follows: [3, 4]

$$\varepsilon'(f) = A.f^{-\frac{3}{2}} + B \qquad \text{(S1)}$$

$$\varepsilon''(f) = C.f^{-1} \qquad \text{(S2)}$$

$$where,\ A = \frac{2nq^2D^{\frac{3}{2}}}{\varepsilon_o\sqrt{\pi}dk_BT},\ B = \varepsilon_\infty \text{ and } C = \frac{2nq^2D}{\varepsilon_o k_BT}$$

From the above-mentioned formula, diffusion coefficient (D) can be calculated as:

$$D = \frac{A^2\pi d^2}{C^2} \qquad \text{(a)}$$

The ion concentration (n) can be calculated as-

$$n = \frac{C\varepsilon_o k_B T}{2q^2 D} \qquad \text{(b)}$$

where n is the ionic concentration, D is the diffusion constant of the ions, q is the electronic charge, k_B is the Boltzmann constant, T is the ambient temperature and d is the thickness of the LC sample cell. Equations (S1) and (S2) did not describe the formation of the electric double layer (EDL); instead, they explained the effect of space charge polarization. The development of the EDL was observed to be strongly dependent on the efficiency of impurity ion adsorption and desorption. [5] The investigation focused on dielectric parameters within the frequency range of 100 Hz to 1 kHz [6, 7]. Typically, liquid crystals contain a notable concentration of free ions, which, in turn, leads to an increase in rotational viscosity. This increase results in a delayed response of the director to an external electric field. However, SnSe NSs dispersed in liquid crystal media function as effective ion traps due to their high ion-trapping constant. The ions become immobilized at the adsorption sites on the NSs. Consequently, when an adequate quantity of SnSe NSs is introduced into the liquid crystal medium, it reduces the free ion concentration, leading to a decrease in the overall rotational viscosity (see Table S1). This hybrid system exhibits enhanced dielectric anisotropy and reduced rotational viscosity, resulting in a faster response to an applied electric field. This accelerated response has promising implications for the development of faster liquid crystal displays (LCDs). In our current study, we also determined the optimal concentration threshold for SnSe NSs, which was found to be 0.5 wt%. Beyond this concentration, the system experienced disruption, aggregation, ion generation rather than trapping, slower switching, reduced birefringence, and a lower order parameter. Our findings indicate that the best results were achieved at the 0.5 wt% concentration, and the corresponding results are presented in Table S1.

Table S1: The fitted values of the constants A, B and C and corresponding calculated values of ionic concentration (n) and diffusion constant (D) of pure and SnSe NSs dispersed NLC cells.

SnSe NSs (wt%)	**A**	**B**	**C**	**n (m^{-3})**	**D (m^2/sec)**
Pure E7	249.26	4.68	651.07	3.74E+19	1.24E-11
0.01	2111.2	4.52	759.95	8.30E+17	6.55E-10
0.05	3127.3	5.36	935.02	7.04E+17	9.50E-10
0.10	5208.3	4.69	1297.3	6.78E+17	1.37E-09

0.30	8518.2	5.28	1748.5	6.21E+17	2.02E-09
0.50	10016	5.30	2208	9.04E+17	1.75E-09

Relaxation Frequency of Flip-Flop Motion:

The Cole-Cole fitting [8] have been performed to calculated the relaxation frequency for flip-flop motion for nematic LC molecule about short molecular axis. Since impurity ions in a nematic LC can cause disruptions or defects in the LC's molecular structure, leading to increased friction and hindered motion of LC molecules. This affects the relaxation frequency, which measures how quickly LC molecules reorient in response to an applied field, making it higher when impurity ions are present. When SnSe NSs are added to the LC, they can interact with and capture the impurity ions, reducing their concentration in the LC. This, in turn, decreases the disruptions and defects in the LC's molecular structure, reducing the friction and hindrance experienced by LC molecules during reorientation. As a result, the relaxation frequency decreases. Figure S9 clearly demonstrates a significant reduction in the relaxation frequency when incorporating the SnSe blend.

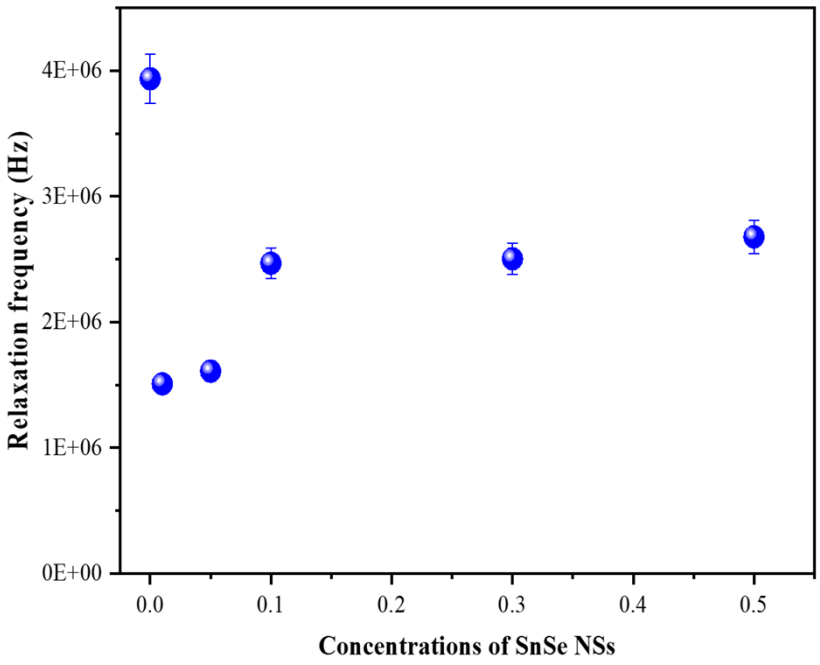

Figure S9: Variation of relaxation frequency of nematic LC molecule about short molecular axis as a function of SnSe NSs concentration.

References:

1. X. Zhao, T. Li, Z. Tang, Y. Li, Y. Miao, H. Xing, M. Cai, X. Wang, X. Kong and W. Ye, *Liquid Crystals*, 2021, **48**, 15-22.

2. H.-Y. Chen, W. Lee and N. A. Clark, *Applied Physics Letters*, 2007, **90**.
3. S. Uemura, *Journal of Polymer Science: Polymer Physics Edition*, 1972, **10**, 2155-2166.
4. S. Uemura, *Journal of Polymer Science: Polymer Physics Edition*, 1974, **12**, 1177-1188.
5. S. P. Yadav, R. Manohar and S. Singh, *Liquid Crystals*, 2015, **42**, 1095-1101.
6. B. P. Singh, C.-Y. Huang, D. P. Singh, P. Palani, B. Duponchel, M. Sah, R. Manohar and K. K. Pandey, *Journal of Molecular Liquids*, 2021, **325**, 115130.
7. B. P. Singh, S. Sikarwar, K. K. Pandey, R. Manohar, M. Depriester and D. P. Singh, *Electronic Materials*, 2021, **2**, 466-481.
8. S. Parab, M. Malik and R. Deshmukh, *Journal of Non-Crystalline Solids*, 2012, **358**, 2713-2722.